Romanian Reports in Physics, Vol. 66, No. 4, P. 1125–1136, 2014

OPERATIONAL PARAMETERS OF THERMAL WATER VAPOR PLASMA TORCH AND DIAGNOSTICS OF GENERATED PLASMA JET*

A. TAMOŠIŪNAS, P. VALATKEVIČIUS, V. GRIGAITIENĖ, V. VALINČIUS

Lithuanian Energy Institute, Plasma Processing Laboratory, Breslaujos str. 3, Kaunas, Lithuania,
E-mail: tamosiunas@mail.lei.lt; pranas@mail.lei.lt; vika@mail.lei.lt; vitas@mail.lei.lt

Received July 30, 2013

Abstract. The operational characteristics of the experimental direct current plasma torch with water vapor stabilization of the arc discharge and diagnostics of generated plasma jet at the nozzle exhaust of the torch were studied in this research. The operation parameters of the torch are presented in terms of generalized thermal and electrical characteristics, which were compared with equations for steam plasma generators. Optical emission spectroscopy (OES) method was used as an important diagnostic tool to investigate the composition of generated plasma jet. The rotational and excitation temperatures of species from the emission spectra were calculated roughly.

Key words: Arc discharge, thermal plasma, water vapor, optical emission spectroscopy.

1. INTRODUCTION

Based on the temperatures of electrons, ions and neutrals, plasmas could be classified as 'thermal' and 'non-thermal'. Thermal plasmas are characterized by high energy density, high temperatures and ability to initiate chemical reactions [1, 2]. Therefore, direct application of thermal plasma generators for industrial and scientific purposes such as metallurgy [3, 4], plasma welding and cutting [5, 6], surface modification of materials including plasma spraying [7, 8] and etc. requires a number of experimental and fundamental analytical investigations to be performed.

In spite of a variety of existing methods to generate thermal plasma by radio frequency, microwaves or electromagnetic induction, the most simple and efficient way is by using an electric arc. Therefore, this experimental research deals with the direct current arc discharge plasma torches.

* Paper presented at the 16th International Conference on Plasma Physics and Applications, June 20–25, 2013, Magurele, Bucharest, Romania.

Since there are quite a lot of experimental and analytical research done for plasma torches operating on air, argon, nitrogen and hydrogen, but it lacks the information about the plasma torches operating on a pure steam or a mixture of gas and steam/water. Recently, the interest has been raised for a broad application of gas-steam or water plasma torches in thermal plasma pyrolysis/gasification of biomass [9, 10], reforming of hydrocarbons [11, 12] and neutralization of hazardous organic compounds [13, 14], as well as production of hydrogen or synthesis gas [15, 16] and formation of hard coatings [17] etc. Due to this, various issues on arc discharge plasma torches, stabilized by vapor or water flux, are extensively studied in more detailed experimental investigations regarding the design, properties and diagnostics of generated plasma jet [18 – 24].

Therefore, the goal of the present experimental research is to determine operational parameters of the thermal water vapor plasma torch operating at atmospheric pressure and compare the results with theoretical, generally used for the steam plasma torches. Moreover, the diagnostics of the generated plasma jet are performed by optical emission spectroscopy method.

2. EXPERIMENTAL SETUP AND METHODOLOGY

2.1. EXPERIMENTAL SETUP

The experiments were performed in plasma torch with stabilization of arc by overheated water vapor up to 450 K. The sketch of the experimental device is shown in Fig. 1. Water vapor with small amount of shielding gas argon was tangentially injected into the arc discharge chamber creating a vortex which surrounds the arc column. A mixture of argon-water vapor was exhausted at the exit nozzle of anode forming a plasma jet. The cathode was made of tungsten-lanthanum rod with 2 mm in diameter embedded into a copper cylinder. A confusor-type stair-shaped anode was used to sustain axial stabilization of the arc and fix the mean arc length suppressing the large-scale shunting. The magnetic coil placed downstream the arc flow was used to minimize anode erosion.

The experiments were performed with the torch power of 45–70 kW, under varying arc current from 160–200 A and flow rate of water vapor from 2.63–4.48 g/s. Mean plasma velocity and temperature at the nozzle exit of anode for these parameters varied between 300 m/s and 2200 K to 600 m/s and 3100 K, respectively.

Dry saturated water vapor was produced by a 5-bar pressure steam generator (GAK-25/50). Before the injection in the discharge chamber it was overheated up to 450 K by means of superheater. This is essential condition avoiding condensation of water vapor on the walls of the discharge chamber. The flow rate rates of plasma forming gas and shielding gas were adjusted by mass flow controllers.

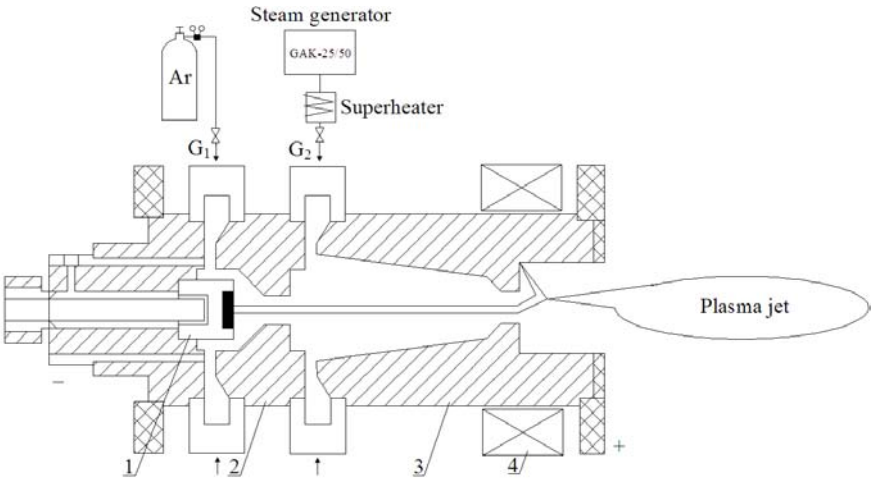

Fig. 1 – The sketch of experimental system; plasma torch: 1 – cathode, 2 – neutral section, 3 – confusor-type stair-step anode, 4 – magnetic coil (solenoid), G_1 and G_2 – gas supply rings.

2.2. METHODOLOGY

The current intensity and the voltage of the arc were measured using a remote control block with voltmeter and ammeter inside connected to the electric power source (VTPE 400-750). The mean temperature and velocity of plasma jet were calculated from the mass balance calculations measuring the power loss to the cooling water by calorimetric method. The electrical and thermal characteristics of the torch were deduced in terms of criteria complexes using a theory of similarity. The obtained experimental results were compared to the fundamental equations describing the electrical and thermal processes in steam plasma torches proposed in [25].

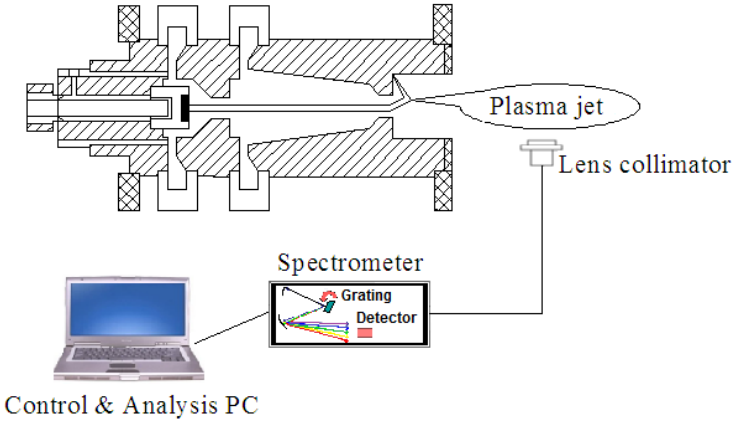

Fig. 2 – The measuring system with an acousto-optic emission spectrometer.

A spectroscopic diagnostics of plasma jet was performed by means of an acousto-optic emission spectrometer (AOS4-1). The measuring system is shown in Fig. 2. The spectrometer with the spectral resolution of 0.05 nm (at 250 nm) and 0.5 nm (at 800 nm) is able to measure radiation emitted from a light source in near UV-VIS spectral range of 250–800 nm wavelength. Time resolution of the spectrometer can vary from 5 to 100 ms. The spectrometer is controlled *via* standard USB 2.0 interface from laptop. The "IntelliSpec" software was used for measurements and manipulation of obtained emission spectra.

3. RESULTS AND DISCUSSION

3.1. OPERATIONAL PARAMETERS OF WATER VAPOR PLASMA TORCH

The most important electrical characteristic of the plasma torch is the volt-ampere characteristic (VAC). The form of this characteristic determines the selection of the parameters of the power source and the electrical efficiency of the torch.

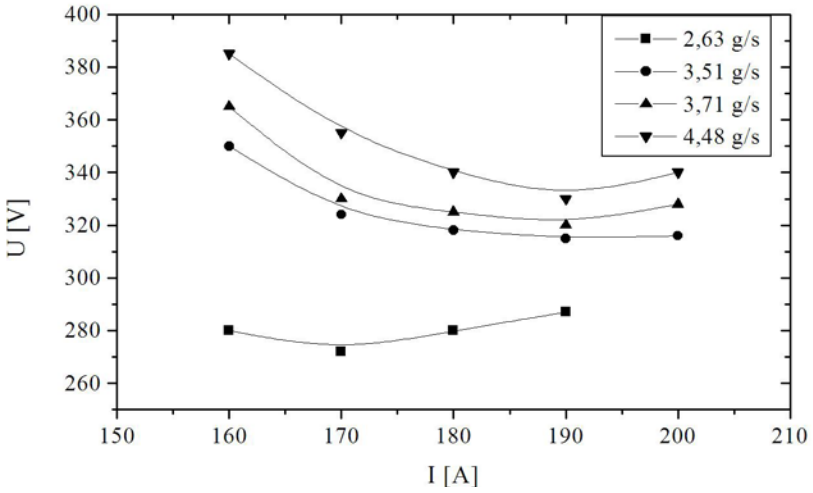

Fig. 3 – Volt-ampere characteristics of the linear water vapor plasma torch.

The drooping VAC creates a certain difficulties by matching the plasma torch with the electric power source. Therefore, a stable arcing is being ensured by inclusion of ballast rheostat in the electrical circuit, which reduces electrical efficiency of the plasma system and initiates the pulsations of arc voltage determined by large-scale shunting. Thus, a stair-step shape of the anode is used to minimize the electrical breakdown between the electrode and the arc in the plasma

torch and to obtain the rising form of volt-ampere characteristics. The form of the VACs of the plasma torch stabilized by water vapor was verified in the range of parameters shown in Fig. 3. The form of VACs is typical for the arc-heated steam plasma source characteristics obtained in [26].

Since the existing analytical methods are not capable to describe the processes occurring in the electric arc plasma torches, we can refer to the theory of similarity to generalize and compare the experimentally obtained results. At present time there are no universal generalized equations valid for all gases, therefore the comparison was made to the generalizing VAC of the arc, burning in water vapor proposed in [25]:

$$U = 70 + 26.4\left(\frac{I^2}{GD}\right)^{-.013} \times \left(\frac{G}{D}\right)^{0.2} \times (pD)^{0.48} \times \left(\frac{L}{D}\right), \tag{1}$$

where U is the voltage, D – the diameter, I – the current intensity, G – the gas flow rate, p – the pressure, L – the mean arc length.

The range of variation of the complexes in the equation is as follows:

$$\begin{aligned} &I^2/GD = (3.0 \div 367)\cdot 10^8\ \mathrm{A^2 s/(kg\times m)},\\ &G/D = 0.017 \div 0.22\ \mathrm{kg/(m\times s)},\\ &pD = (1.7 \div 4.9)\cdot 10^3\ \mathrm{N/m},\\ &L/D = 4.1 \div 13.5. \end{aligned} \tag{2}$$

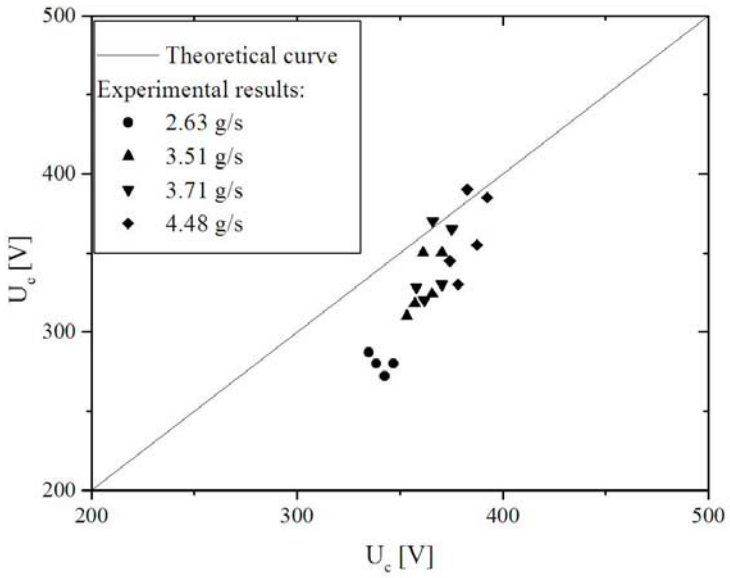

Fig. 4 – Comparison of the experimental data with the generalized volt-ampere characteristic of the arc burning in water vapor, U_e – experimental results, U_c – calculated according to Eq. (1).

One can see than the flow rate of water vapor is 2.63 g/s, the scatter of the experimental results differs from calculated in more than 18%. This could be explained by the effect of supplying shielding gas argon. According to [25], the presence of argon may decrease the arc voltage by 1/3 if the amount of this shielding gas is more than 25% in the total flow rate. In this case, the amount of argon was 17%. Moreover, argon has a higher conductivity in comparison with water vapor. Therefore, growth in the ratio of argon results in a voltage decrease. The best agreement was obtained than the flow rate of water vapor varied from 3.71 to 4.48 g/s with difference between the U_c and U_e voltages less than 10%.

Thermal coefficient of the efficiency of the plasma torch stabilized by water vapor vortex was determined by processes proceeding in the column of the electric arc taking into account the heat exchange between the arc, the heated gas and the walls of the discharge chamber. The methodology describing thermal efficiency of the torch is proposed in detail [25]. Therefore, the integral coefficient of heat transfer of the steam plasma torches may be expressed as follows:

$$\tilde{\eta} = \frac{1-\eta}{\eta} = 3.02 \cdot 10^{-6} \left(\frac{I^2}{GD}\right)^{0.32} \times \left(\frac{G}{D}\right)^{-0.57} \times (pD)^{0.4} \times \\ \times \left(1 + 1.2K_y\right)\left(1 + \mathrm{tg}(\alpha/2)\right)(L/D)^{0.5}, \tag{3}$$

where: η is the thermal efficiency of the plasma torch, I – the current intensity, G – the gas flow rate, D – the diameter, L – the mean arc length. If there is a ledge in anode, than $K_y = 1$, with no ledge, $K_y = 0$.

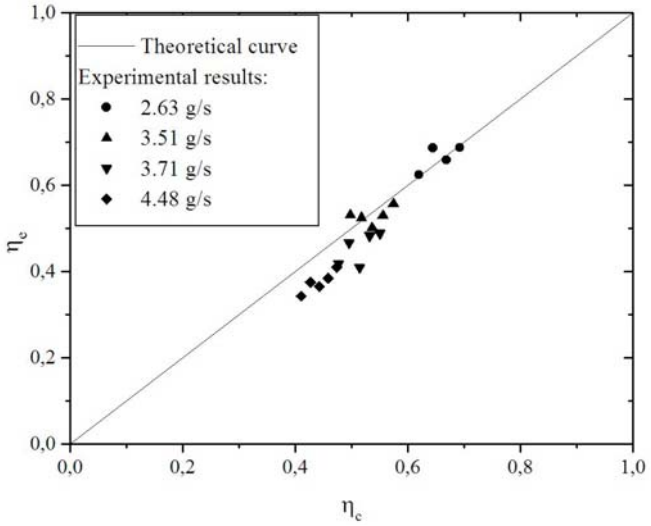

Fig. 5 – Comparison of the experimental (η_e) and calculated (η_c) values of the thermal efficiency for the water vapor plasma torch.

Experimental results illustrated in Fig. 5 show a good correspondence with accuracy less than 7% from the calculated data according to Eq. (3). Moreover they are close to the data measured in [25]. It could be assumed that the integral heat losses in the plasma torch are reduced due to the increased flow rate of water vapor from 2.63 to 4.48 g/s, which has an impact on the increment of boundary layer of cold gas surrounding the electric arc and serving as a screen from the convective and radiant heat flux to the walls of the discharge chamber. Therefore, thermal efficiency of the plasma torch increases reaching the maximum value of $\eta = 0.75$.

3.2. DIAGNOSTICS OF GENERATED PLASMA JET

3.2.1. Identification of species in the emission spectra

The emission spectra of the DC arc plasma stabilized by a mixture of argon-water vapor at atmospheric pressure are shown in Figs. 6 and 7. The spectra were measured in the range of wavelength from 300 to 800 nm at flow rate of water vapor 3.71 g/s. As could be seen in both figures, between 550 nm and 650 nm there was a noise coming from outside which could cause the errors calculating temperature of species in the plasma [27]. The noise could appear due to high-velocity flow (up to 700 m/s) of plasma stream at the nozzle exhaust of the torch and the fluctuations of the arc. Thus, it may affect the precision of the spectra measurements. Moreover, resolution of the spectrometer is an important factor which could influence inaccuracies in spectra too.

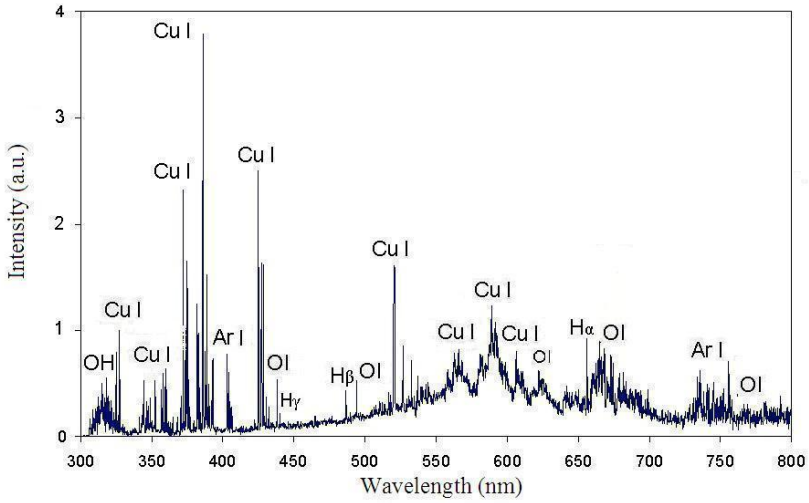

Fig. 6 – Optical emission spectra of water vapor plasma at torch power of 47.6 kW (170 A, 280 V).

The optical emission spectrum shows that water molecule in the plasma was decomposed into H, OH and O radicals as it was confirmed in [28]. The main emission lines include Ar (I), OH, O (I), Cu (I), and Balmer emission line profile corresponding to H_α, H_β and H_γ were detected. These lines along with their spectroscopic parameters were taken from the NIST atomic database [29]. The peaks of H_α and H_β in the emission profile suggest that slow hydrogen atoms with low average energies of 0.4–1 eV were dominant [30], and only traces of H_γ were detected. Heating mechanism of plasma stream is induced mainly by elastic collision between heavy ions and fast electrons.

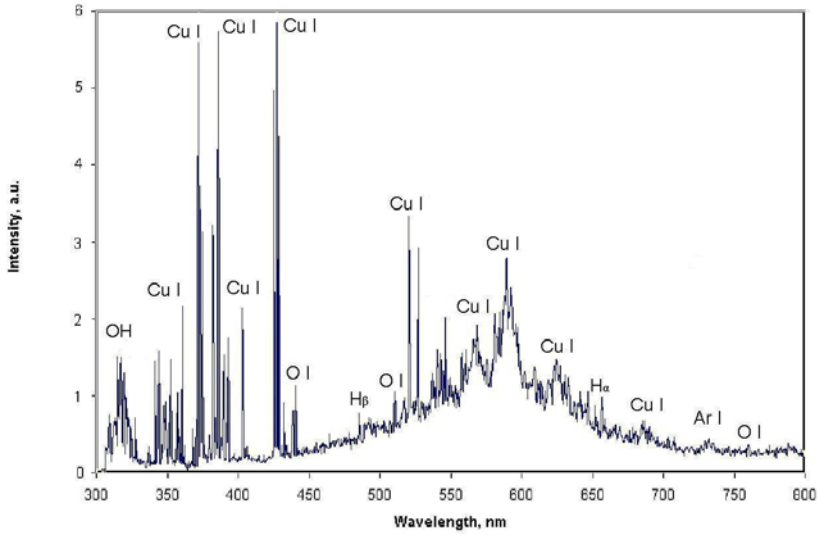

Fig. 7 – Optical emission spectra of water vapor plasma at torch power of 62 kW (250 A, 248 V).

High currents are important to produce active species in plasma (especially OH, H, O radicals) which are very beneficial in reforming, pyrolysis and gasification of organic waste extracting hydrogen rich synthesis gas or producing other chemicals. On the other hand, the increase of the current increases the emission of Cu I atoms from the anode surface to the plasma. Thus, the life-time of the electrodes decreases due to intensive erosion.

3.2.2. Temperature evaluation from the emission spectra

The OH (A-X) band spectra have been used to calculate the gas temperature [31]. It enabled to determine rotational T_{rot} temperature ($T_{rot} \approx T_g$) by fitting the experimental spectra with simulated one. We used LIFBASE [32] software for spectral simulation.

To find out whether the rotational temperature determined from the measured spectra was reliable, it was compared with the mean gas temperature at the nozzle

exhaust of the torch calculated from a heat balance equations ($T_{balance}$) [25]. The results are shown in Table 1. It could be seen that at current intensities of 170 A and 250 A, the difference between the temperatures ($T_{balance}$ and T_{rot}) was significant. The mean temperature increased with increasing the current intensity because of Joule heating of the gas, i.e. high densities of active species are being generated in the plasma with fast interspecies collisional exchange [33]. Difference between the temperatures may appear due to water vapor used as plasma-forming gas. At temperature 2500 K only 10 % of water vapor dissociated [34] and thus undissociated water vapor causes measurement uncertainty in spectra measurements. In the very humid environment, some portion of energy was spent for water evaporation and dissociation. It was reported in [35] that when no water was present in the discharge, the same discharge at approximately the same parameters gave higher temperatures. In case of experimental temperature 3100 K around 40 % of water vapor dissociated [34]. The T_{rot} was much higher than $T_{balance}$. It could be explained that the rotational temperature measured from OH spectra may be overestimated due to the fact that these radicals are result of chemical reactions and residual chemical energy can manifest itself by elevating temperatures [36].

Table 1

Experimental and calculated results

I [A]	U [V]	P [kW]	G_{H2O} [g/s]	$T_{balance}$ [K]	T_{rot} [K]	T_{exc}[K]
170	280	47.6	3.71	2500±6%	~1700	~4000
250	250	62	3.71	3100±6%	~4600	~4800

Considering that our atmospheric pressure plasma was close to local thermodynamic equilibrium (LTE), the distribution of atoms in different excited states could be described by the Boltzmann distribution function. Therefore, the excitation temperature was roughly calculated using two-line method (considering Cu I line transitions between 510.554 nm and 515.324 nm, as well as among 515.324 nm and 521.820 nm – see Table 2). The relative intensity between two spectral lines of the same species corresponding to transitions j and k to the same lower level i can be expressed as [37, 38]:

$$\frac{I_{ji}}{I_{ki}} = \left(\frac{A_{ji} g_j \lambda_{ki}}{A_{ki} g_k \lambda_{ji}} \right) \exp\left\{ -\frac{E_{ji} - E_{ki}}{kT_{exc}} \right\}, \tag{4}$$

where I_{ji} and I_{ki} is the line intensities from the j–i and k–i transitions, λ_j and λ_k – the wavelengths, A_{ji} and A_{ki} the transition probabilities, E_{ji} and E_{ki} the energy differences between the exited levels j and k and the level i, g_j and g_k the degeneracy of the levels j and k, T_{exc} the excitation temperature and k_B is the Boltzmann constant.

Table 2

Line parameters of the Cu I lines [33]

Line	λ [nm]	E_i [eV]	E_j [eV]	g_i	g_j	A_{ij} [10^8 s^{-1}]
Cu I	510.554	3.817	1.389	4	6	0.02
Cu I	515.324	6.191	3.786	4	2	0.6
Cu I	521.820	6.192	3.817	6	4	0.75

The evaluated excitation temperatures (see Table 1) are quite in a good agreement with other author who investigated a similar discharge at atmospheric pressure [39]. At current intensity of 170 A, a difference between the rotational and excitation temperatures was significant. It indicated that our plasma was not in a local thermal equilibrium (LTE). The same explanation described previously may stand commenting on this difference. In opposite, at current intensity of 250 A the obtained rotational and excitation temperatures ($T_{rot} \approx T_{exc}$) were close to each other indicating that the local thermodynamic equilibrium conditions in our plasma were fulfilled. According to [40] the atmospheric DC arc plasmas are supposed to reach a LTE.

Finally, it is important to note that the rotational and excitation temperatures determined from the measured spectra were calculated roughly. Thus, more detailed examinations are required considering the estimation of rotational, excitation and electron temperatures, as well as electrons concentration. However, the former temperatures of the DC arc plasma in a mixture of Ar–H_2O vapor are not properly studied and reported in the available literature.

4. CONCLUSIONS

In this research the operational parameters of the atmospheric pressure DC arc plasma torch stabilized with water vapor vortex, as well as diagnostics of generated plasma jet by means of optical emission spectroscopy were studied.

The shielding gas argon was found to reduce the arc voltage by 18% at flow rate of water vapor of 2.63 g/s, while at increased content from 3.71 to 4.48 g/s, a good agreement between the experimental and calculated values has been observed. The experimentally obtained integral coefficient of thermal efficiency of the torch showed a good correspondence with accuracy less than 7% with the calculated data.

An optical emission spectroscopy method was used to determine species in argon-water vapor plasma, as well as the rotational and excitation temperatures. The main emission lines observed were as follows: Ar (I), OH, O (I), Cu (I), and Balmer emission line profile corresponding to H_α, H_β and H_γ. The emission of OH band was used to measure the rotational temperature corresponding to gas temperature. The determined temperatures from the spectra at different

experimental conditions were compared with the mean gas temperatures calculated from a heat balance equations. The rotational temperature was measured to be ~ 1700 K at 47.6 kW, and ~ 4600 K at 62 kW torch power. The excitation temperature was calculated using two-line method from Cu I line transitions between 510.554 nm and 515.324 nm, as well as among 515.324 nm and 521.820 nm. It was found to be in the range of ~ 4000–4800 K. At the plasma torch power of 62 kW, and the current intensity of 250 A, the rotational and excitation temperatures (T_{rot} and T_{exc}) were close to each other indicating a LTE in the plasma.

Since there is lack of data published on diagnostics of DC arc thermal plasmas in a mixture of Ar–water vapor by optical emission spectroscopy estimating temperatures from the measured spectra, more detailed examinations are required considering this issue.

Acknowledgments. This research was funded by a grant (no. ATE-10/2012) from the Research Council of Lithuania.

REFERENCES

1. C. Tendero, Ch. Tixier, P. Tristant, J. Desmaison, Ph. Leprince, Spectrochim. Acta B., **61**, 2–30 (2006).
2. G. Bonizzoni, E. Vassallo, Vacuum, **64**, 327–336 (2002).
3. M. I. Boulas, P. Fauchais, E. Pfender, *Thermal Plasmas: Fundamental and Applications*, Plenum Press, New York, 1994.
4. E. Pfender, Pure Appl. Chem., **60**, 519–606 (1988).
5. A. I. Al-Shamma'a, S. R. Wylie, J. Lucas, R. A. Stuart, Process. Technol., **121**, 143–147 (2002).
6. W. J. Xu, J. C. Fang, X. S. Lu, J. Mater. Process. Technol., **129**, 152–156 (2002).
7. P. Fauchais, A. Vardelle, A. Denoirjean, Surf. Coat. Technol., **97**, 66–78 (1997).
8. V. Snapkauskiene, V. Valincius, P. Valatkevicius, Catal. Today, **176**, 77–80 (2011).
9. Ph. G. Rutberg, V. A. Kuznetsov, E. O. Serba, S. D. Popov, A. V. Surov, G. V. Nakonechny, A. V. Nikonov, Appl. Energ., **108**, 505–514 (2013).
10. G. Van Oost, M. Hrabovsky, V. Kopecky, M. Konrad, M. Hlina, T. Kavka, Vacuum, **83**, 209–212 (2008).
11. G. Ni, Y. Lan, Ch. Cheng, Y. Meng, X. Wang, Int. J. Hydrogen Energ., **36**, 12869–12876 (2011).
12. S. Ch. Kim and Y. N. Chun, Int. J. Hydrogen Energ., **13**, 523–529 (2007).
13. D. Y. Kim, D. N. Park, Surf. Coat. Techn., **202**, 5280–5283 (2008).
14. T. Watanabe, T. Tsuru, Thin Solid Films, **516**, 4391–4396 (2008).
15. Y. Byun, M. Cho, J. W. Chung, W. Namkung, H. D. Lee, S. D. Jang, Y. S. Kim, J. H. Lee, C. R. Lee, S. M. Hwang, J. Hazard. Mater., **190**, 317–323 (2011).
16. S. C. Kim, Y. N. Chun, Renew. Energ., **33**, 1564–1569 (2008).
17. G. Espie, A. Denoirjean, P. Fauchais, J. C. Lable, J. Dulsky, O. Schneeweiss, K. Volenik, Surf. Coat. Techol., **195**, 17–28 (2005).
18. A. Tamosiunas, V. Grigaitiene, P. Valatkevicius, Nukleonika, **56**, 131–135 (2011).
19. M. Hrabovsky, Pure Appl. Chem., **70**, 1157–1162 (1998).
20. M. Hrabovsky, Pure Appl. Chem., **74**, 429–433 (2002).
21. M. Hrabovsky, M. Konrad, V. Kopecky, V. Sember, Ann. NY. Acad. Sci., **891**, 57–63 (1999).
22. B. Glocker, G. Nentwig, E. Messerschmid, Vacuum, **59**, 35–46 (2000).

23. G. Ni, P. Zhao, Ch. Cheng, Y. Song, H. Toyoda, Y. Meng, Plasma Sources Sci. Technol., **21**, 015009 (2012).
24. L. Tiaming, S. Choi, T. Watanabe, Plasma Sci. Technol., **14**, 1097–1101 (2012).
25. M. F. Zhukov, *Thermal Plasma Torches: Design, Characteristics, Applications*, Cambridge International Science Ltd, 2007, p. 596.
26. S. W. Kim, H. S. Park, H. J. Kim, Vacuum, **70**, 59–66 (2003).
27. C. Trassy, A. Tazeem, Spectrochim. Acta B, **54**, 581–602 (1999).
28. N. G. Hua, M. Y. Dong, Ch. Cheng, L. Yan, Chinese Phys. Lett., **27**, 055203 (2010).
29. *** NIST Atomic Spectra Database, http://physics.nist.gov
30. R. L. Mills, B. Dhandapani, K. Akhtar, Int. J. Hydrogen Energ., **33**, 802–815 (2008).
31. D. A. Levin, Ch. Laux, Ch. H. Kruger, J. Quant. Spectrosc. Radiant. Transfer, **61**, 377–392 (1999).
32. J. Luque, D.R. Crosley, LIFBASE: Database and Spectral Simulation (version 1.5), SRI International Report, MP 99–009 (1999).
33. B. N. Sismanoglu, J. Amorim, J. A. Souza-Correa, C. Oliveira, M. P. Gomes, Spectrochim. Acta B, **64**, 1287–1293 (2009).
34. N. B. Vargaftik, Thermophysical properties of gases and liquids (in Russian), Nauka, Moscow, 1972.
35. Z. Machala, M. Janda, K. Hensel, I, Jedlovsky, L. Leštinska, V. Foltin, V. Martisovitš, M. Morvova, J. Mol. Spectrosc., **243**, 194–201 (2007).
36. D. Staack, B. Farouk, A. Gutsol, A. Fridman, Plasma Sources Sci. Technol., **14**, 700–711 (2005).
37. M. M. Larijani, F. Le Normand, O. Cregut, Appl. Surf. Sci, **253**, 4051–4059 (2007).
38. D. Liu, Y. Xu, X. Yang, Sh. Yu, Q. Sun, A. Zhu, T. Ma, Diam. Relat. Mater., **11**, 1491–1495 (2002).
39. T. Li, S. Choi, T. Watanabe, T. Nakayama, T. Tanaka, Thin Solid Films, **523,** 72–75 (2012).
40. A. Schutze, J. Y. Jeong, S. E. Babayan, J. Park, G. S. Selwyn, R. F. Hicks, IEEE T. Plasma Sci., **26**, 1685–1692 (1998).